Fetal Diagnosis and Therapy

Research Article

Fetal Diagn Ther 2021;48:235–242
DOI: 10.1159/000512689

Received: September 14, 2020
Accepted: October 28, 2020
Published online: March 17, 2021

Prenatal Imaging Diagnosis of Suprarenal Lesions

Stefanie P. Lazow[a] Danielle M. Richman[b] Beatrice Dionigi[a, c] Steven J. Staffa[d] Carol B. Benson[b] Terry L. Buchmiller[a]

[a]Department of Surgery, Boston Children's Hospital/Harvard Medical School, Boston, MA, USA; [b]Department of Radiology, Brigham and Women's Hospital/Harvard Medical School, Boston, MA, USA; [c]Department of Surgery, Cleveland Clinic, Cleveland, OH, USA; [d]Department of Anesthesiology, Critical Care and Pain Medicine Research, Boston Children's Hospital/Harvard Medical School, Boston, MA, USA

Keywords
Suprarenal · Adrenal · Prenatal · Sequestration · Adrenal hemorrhage

Abstract
Introduction: Prenatal suprarenal lesions represent diverse pathologies. This study investigated prenatal imaging features and regression patterns associated with specific lesion diagnoses. ***Methods:*** This is a multicenter retrospective review of fetuses with prenatally diagnosed suprarenal lesions between 2001 and 2019. Prenatal ultrasound and MRI characteristics, postnatal imaging, and clinical course were reviewed. Prenatal imaging findings were compared by the most common diagnoses and regression patterns. ***Results:*** Forty-four fetuses were prenatally diagnosed with suprarenal lesions. Diagnoses included pulmonary sequestration (n = 12; 27.3%), adrenal hemorrhage (n = 12; 27.3%), upper quadrant cyst (including 2 duplication cysts, 1 splenic cyst, and 3 indeterminate cysts), neuroblastoma (n = 4), adrenal hyperplasia (n = 3), bilateral adrenal calcifications (n = 1), and indeterminate lesions (n = 6). Sequestrations were uniformly left-sided (100 vs. 50%; p = 0.014) and diagnosed earlier in gestation than adrenal hemorrhages (p = 0.025). Sequestrations were also significantly more likely to have a prenatal feeding vessel (p = 0.005), low T1 MRI signal (p = 0.015), and no MRI blood products (p = 0.018) compared to adrenal hemorrhages. When comparing all 44 patients, a prenatal feeding vessel and low T1 signal on prenatal MRI were significantly associated with lesion persistence (p = 0.003; p = 0.044). ***Discussion/Conclusion:*** Imaging findings on prenatal ultrasound and MRI aid in the diagnosis of suprarenal lesions, including differentiating pulmonary sequestrations and adrenal hemorrhages.

Introduction

With improved prenatal imaging techniques, fetal abdominal lesions, including in the suprarenal region, are detected prenatally with increasing frequency [1, 2]. The differential diagnosis for a suprarenal lesion is broad, ranging from benign to malignant pathologies. Possible diagnoses include adrenal hemorrhage [3, 4], infradiaphragmatic extralobar pulmonary sequestration [5–7], gastrointestinal duplication cyst [8], and neuroblastoma [8, 9]. The expected clinical trajectory of these lesions is diverse, ranging from undergoing complete regression to requiring postnatal resection [6, 8, 10]. Despite improvements in prenatal ultrasound and increased utilization of prenatal MRI, the use of radiological findings to reliably distinguish between these different diagnoses remains challenging [10–12].

karger@karger.com
www.karger.com/fdt

Terry L. Buchmiller
Department of Surgery, Boston Children's Hospital
300 Longwood Ave., Fegan 3
Boston, MA 02115 (USA)
terry.buchmiller@childrens.harvard.edu

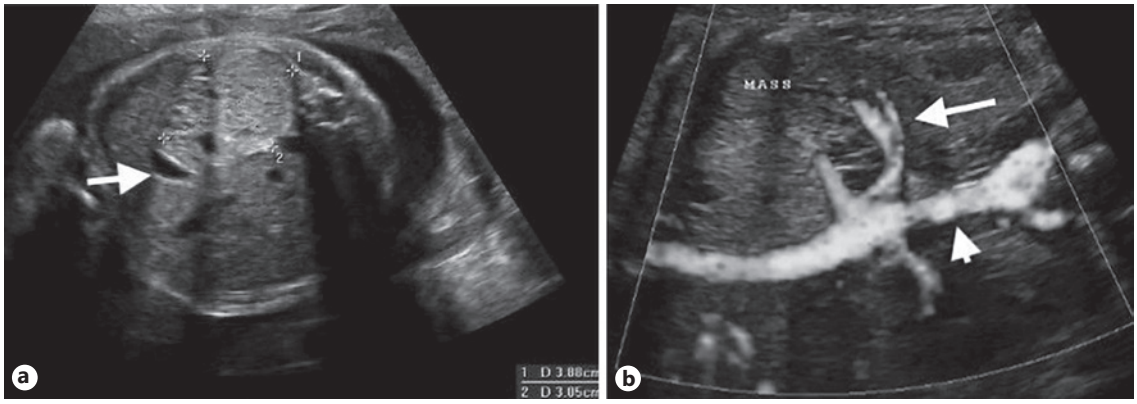

Fig. 1. Infradiaphragmatic sequestration. **a** Transverse gray scale image of a 3.9 cm echogenic mass (calipers) in the left upper quadrant displacing the stomach anteriorly (arrow). **b** Sagittal power gray-scale Doppler image of the left upper quadrant mass (labeled mass) with a feeding vessel (arrow) arising from the aorta (arrowhead).

Therefore, the primary goal of this study was to investigate if any prenatal imaging findings are associated with specific suprarenal lesion diagnoses and to assess lesion regression patterns. This would potentially enable improved prenatal counseling regarding the expected clinical course of the prenatally diagnosed suprarenal lesion.

Materials and Methods

This study is an IRB-approved 2-center retrospective review of fetuses diagnosed on prenatal ultrasound with a suprarenal lesion from 2001 to 2019. Prenatal imaging was performed at one or both of the 2 centers (the Maternal Fetal Care Center at Boston Children's Hospital or Brigham and Women's Hospital). For fetuses with lesions that did not regress prenatally, postnatal imaging follow-up at Boston Children's Hospital was required to be included in this study. For lesions that regressed prenatally, postnatal follow-up was not required for inclusion.

Baseline clinical variables collected via chart review included fetus sex, maternal age, and any associated anomalies. Prenatal imaging features were collected from all prenatal ultrasounds as well as prenatal MRI if available. Gestational age at first abnormal prenatal ultrasound and the number of subsequent prenatal ultrasounds were recorded. Ultrasound findings included lesion laterality, composition, echogenicity, and maximum dimension on the first abnormal prenatal ultrasound. If bilateral lesions were present, the maximum dimension of the largest lesion was used in analysis. Prenatal MRI findings included high or low T1 and T2 signal as well as the presence of blood products. The presence of a prenatal feeding vessel was based upon identification on either ultrasound with Doppler or MRI.

If tissue pathology was available from lesion biopsy or surgical resection, then the pathology report was used to assign a diagnosis. If tissue pathology was not available, lesions were assigned a diagnosis based upon the clinically assigned diagnosis, which was determined from prenatal and postnatal imaging reports as well as clinical notes. Cysts located in the upper quadrant without a definitive diagnosis were classified as "upper quadrant cysts." Lesions without a specific imaging appearance were classified as "indeterminate."

The size of the lesion was followed on prenatal and postnatal imaging. Specifically, the prenatal evolution of lesion size was categorized based upon changes in lesion maximum dimension between the first and last prenatal ultrasound. Similarly, the postnatal evolution of lesion size was evaluated based upon changes in lesion maximum dimension between the first and last postnatal ultrasound. An increase in size was defined as ≥20% increase in maximum dimension, a decrease in size was defined as ≥20% decline, and stable was defined as <20% change. Complete prenatal lesion regression was defined as regression during the prenatal period based on prenatal follow-up ultrasound. Lesions that were present on the last prenatal imaging but had undergone regression by the first postnatal imaging were categorized as undergoing postnatal regression. Lesions that were present at the first postnatal imaging were followed up until they regressed (categorized as postnatal regression), underwent therapy or surgical resection, or were lost to follow-up. Tissue pathology was recorded when available after lesion biopsy or surgical resection. Survival at the last follow-up was recorded.

Statistical Analysis

The nonparametric Wilcoxon rank-sum test and Fisher's exact test were used, as appropriate, to compare prenatal imaging features between lesions by assigned diagnoses, prenatal size evolution, and regression patterns. Kaplan-Meier curves demonstrated the probability of experiencing lesion regression (either prenatal or postnatal). Log-rank testing was then performed to compare the probability of regression (either prenatal or postnatal) in lesions with and without a prenatal feeding vessel. Statistical analyses were performed using Stata version 15.0 (StataCorp, College Station, TX, USA). A 2-sided p value ≤0.05 was considered statistically significant.

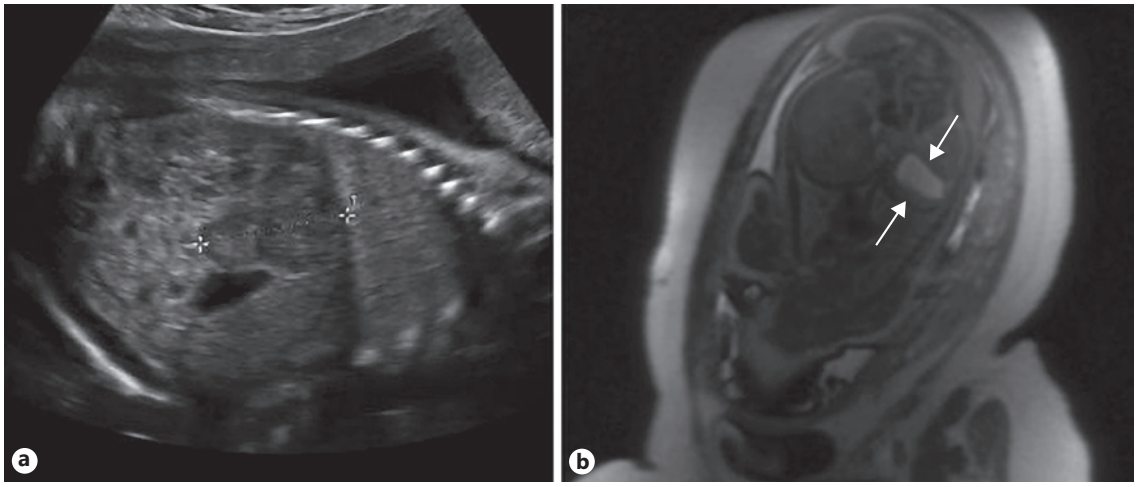

Fig. 2. Adrenal hemorrhage. **a** Sagittal gray-scale ultrasound image of a heterogeneous mass in the left upper quadrant (calipers). **b** T1-weighted MRI of the fetus demonstrating a hyperintense left suprarenal lesion (arrows).

Results

The study included 44 fetuses diagnosed with suprarenal lesions on prenatal ultrasound. Twenty-four (54.5%) fetuses were male. Median maternal age was 31 years (IQR: 26, 35). Associated abnormalities (which were not mutually exclusive) were present in 10 (22.7%) fetuses including renal vein or inferior vena cava thrombosis (n = 4; 9.1%), musculoskeletal anomalies (n = 2; 4.5%), neurological anomalies (n = 2; 4.5%), genitourinary anomalies (n = 1; 2.3%), liver lesions (n = 1; 2.3%), and splenomegaly (1; n = 2.3%). All cases of venous thrombosis were associated with adrenal hemorrhage diagnoses.

Of the 44 fetuses, 30 (68.2%) had left-sided lesions, 9 (20.5%) had right-sided lesions, and 5 (11.4%) had bilateral lesions. Median gestational age at first abnormal prenatal ultrasound was 24.0 weeks (IQR: 19.0, 31.3). Fetuses underwent a median 1.5 (IQR: 1.0, 3.0) prenatal ultrasounds after the first abnormal ultrasound. Median maximum lesion dimension on first abnormal prenatal ultrasound was 16 mm (IQR: 11, 28). Thirty-two (72.7%) fetuses underwent prenatal MRI imaging.

Prenatal Imaging Features by Diagnosis

The most common assigned prenatal diagnoses were pulmonary sequestration (n = 12; 27.3%; shown in Fig. 1) and adrenal hemorrhage (n = 12; 27.3%; shown in Fig. 2). Other diagnoses included upper quadrant cyst (n = 6, including 2 duplication cysts, 1 splenic cyst, and 3 indeterminate cysts, all left-sided) (shown in Fig. 3), neuroblastoma (n = 4), adrenal hyperplasia (n = 3), bilateral adrenal calcifications (n = 1), and indeterminate lesion (n = 6). Tissue pathology was confirmed in 6 lesions after surgical resection, including 2 gastrointestinal duplication cysts, 1 neuroblastoma, and 3 pulmonary sequestrations. An additional lesion was diagnosed as neuroblastoma on biopsy and treated with chemotherapy. Prenatal imaging features for all diagnosis categories in all 44 lesions are detailed in on-

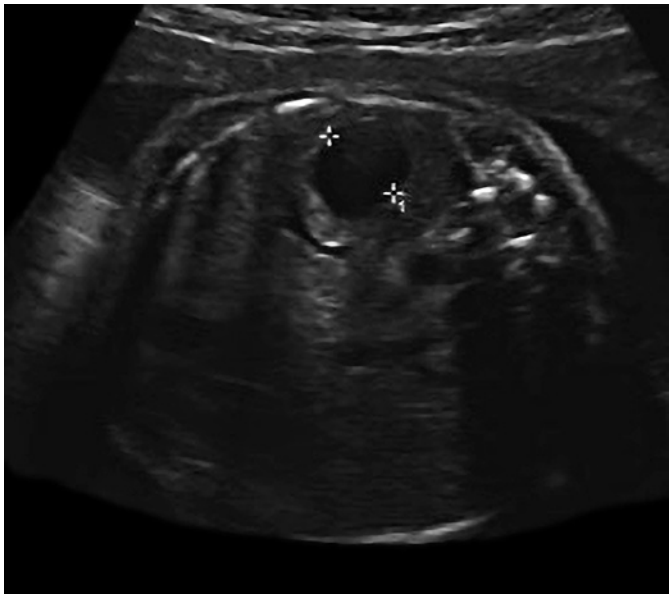

Fig. 3. Left upper quadrant cyst. Transverse gray-scale image with an anechoic cyst in the left upper quadrant (calipers).

Table 1. Prenatal imaging findings by most common diagnoses

	Adrenal hemorrhage (n = 12)	Pulmonary sequestration (n = 12)	p value
Lesion laterality, n (%)			
Right	4 (33.3)	0 (0)	
Left	6 (50.0)	12 (100.0)	0.014*
Bilateral	2 (16.7)	0 (0)	
Gestational age at first abnormal prenatal ultrasound, weeks	27 (21, 34)	20 (18, 23)	0.025*
First prenatal ultrasound maximum dimension, mm	18 (11, 30)	17 (16, 24)	0.868
Feeding vessel, n (%)			
Yes	0/11 (0)	7 (58.3)	0.005*
No	11/11 (100.0)	5 (41.7)	
Composition on ultrasound, n (%)			
Solid	0/11 (0)	7 (58.3)	
Cystic	8/11 (72.7)	2 (16.7)	0.005*
Mixed	3/11 (27.3	3 (25.0)	
Echogenicity on ultrasound, n (%)			
Anechoic	3/11 (27.3)	0 (0)	
Hypoechoic	2/11 (18.2)	1 (8.3)	0.014*
Echogenic	1/11 (9.1)	8 (66.7)	
Mixed	5/11 (45.5)	3 (25.0)	
MRI T1 signal, n (%)			
Low	1/5 (20.0)	6/6 (100.0)	0.015*
High	4/5 (80.0)	0/6 (0)	
MRI T2 signal, n (%)			
Low	1/6 (16.7)	0/8 (0)	0.429
High	5/6 (83.3)	8/8 (100.0)	
MRI blood products, n (%)			
Yes	4/8 (50.0)	0/11 (0)	0.018*
No	4/8 (50.0)	11/11 (100.0)	

Data are presented as n (%) or median (interquartile range). Denominators are presented for variables with missing data. p values were calculated using Fisher's exact test or the Wilcoxon rank-sum test. * Statistically significant at $p \leq 0.05$.

line suppl. Table 1 (for all online suppl. materials, see www.karger.com/doi/10.1159/000512689). For the 7 lesions with confirmed tissue pathology, prenatal imaging findings by tissue diagnosis are detailed in online suppl. Table 2.

Prenatal imaging findings for the most common assigned prenatal diagnoses, pulmonary sequestration and adrenal hemorrhage, were then compared with univariate analysis (Table 1). Compared to adrenal hemorrhages, pulmonary sequestrations were uniformly left-sided (100 vs. 50%; $p = 0.014$) and diagnosed significantly earlier in gestation (median 20 vs. 27 weeks; $p = 0.025$). Pulmonary sequestrations were also significantly more likely to have a prenatal feeding vessel ($p = 0.005$), solid composition ($p = 0.005$), echogenic appearance ($p = 0.014$), low T1 MRI signal ($p = 0.015$), and no MRI blood products ($p = 0.018$) compared to adrenal hemorrhages.

Lesion Evolution

The prenatal evolution of lesion size was analyzed in 39 fetuses with multiple prenatal sonograms with available measurements. Of these, 17 (43.6%) increased in size, 14 (35.9%) were stable, 2 (5.1%) decreased in size, and 6 (13.6%) fully regressed in utero. Median time to prenatal regression after initial diagnosis was 9 weeks (IQR: 2.5, 21.3). In utero evolution was not associated with likelihood of postnatal regression pattern in the 33 fetuses without prenatal regression ($p = 0.999$).

Postnatal follow-up was not available in 4 children with prenatal regression. In the 40 children with postnatal follow-up imaging, median duration of postnatal follow-up was 30.5 months (IQR: 5.8, 62.0) with a median 3.0 postnatal ultrasounds (IQR 1.3, 5.0). Of the 40 children, 39 (97.5%) were alive at last follow-up and 1 had died sec-

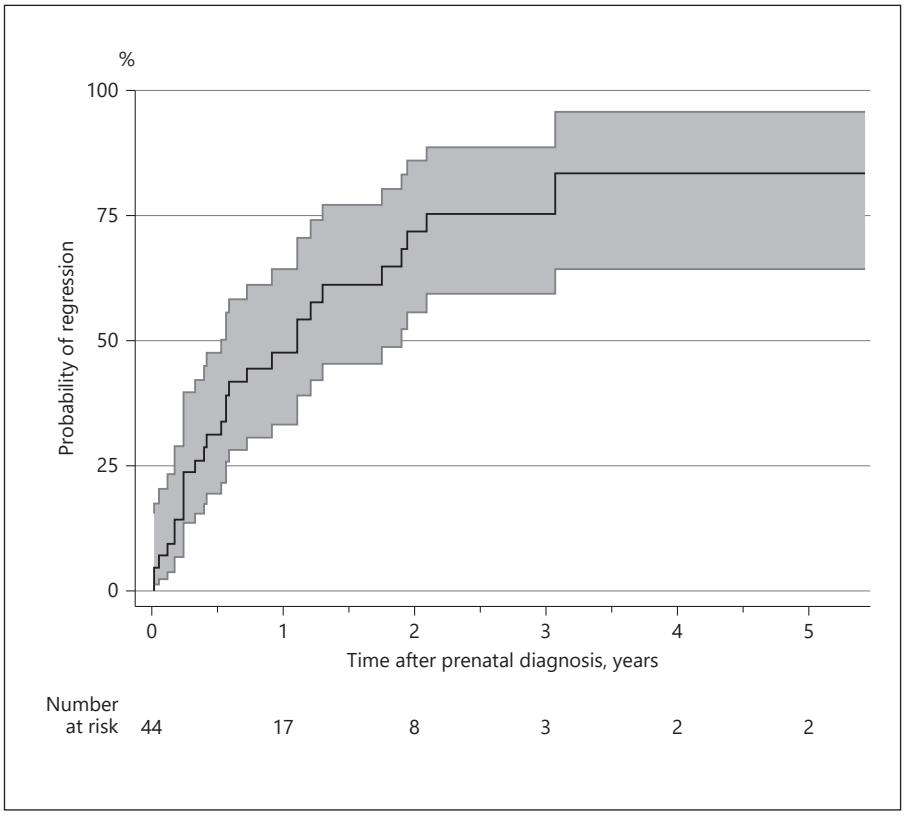

Fig. 4. This Kaplan-Meier curve demonstrates the probability of experiencing lesion regression over time after the prenatal diagnosis with 95% confidence intervals depicted.

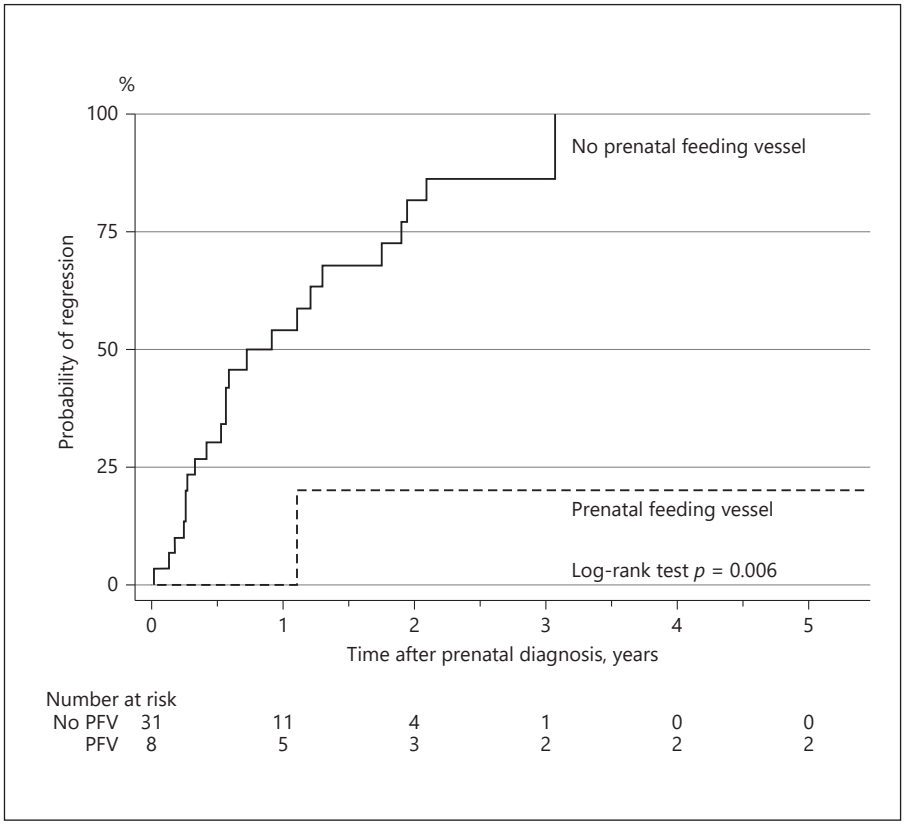

Fig. 5. These Kaplan-Meier curves compare the probability of experiencing lesion regression over time after the prenatal diagnosis between lesions with (black line) and without (dashed line) a PFV on ultrasound or MRI imaging. Log-rank testing demonstrates significantly increased probability of regression in lesions without a PFV ($p = 0.006$). PFV, prenatal feeding vessel.

Table 2. Prenatal imaging findings by lesion regression pattern

Variable	Regression (n = 28)	No regression (n = 16)	p value
Lesion laterality, n (%)			
Right	7 (25.0)	2 (12.5)	
Left	16 (57.1)	14 (87.5)	0.077
Bilateral	5 (17.9)	0 (0)	
Gestational age at first abnormal prenatal ultrasound, weeks	26 (20, 31)	22 (18, 30)	0.486
First prenatal ultrasound maximum dimension, mm	25 (16, 30)	17 (13, 29)	0.213
Feeding vessel, n (%)			
Yes	1/24 (4.2)	7/15 (46.7)	0.003*
No	23/24 (95.8)	8/15 (53.3)	
Composition on ultrasound, n (%)			
Solid	4/23 (17.4)	7 (43.8)	
Cystic	14/23 (60.9)	6 (37.5)	0.242
Mixed	5/23 (21.7)	3 (18.8)	
Echogenicity on ultrasound, n (%)			
Anechoic	7/23 (30.4)	3/15 (20.0)	
Hypoechoic	5/23 (21.7)	1/15 (6.7)	0.380
Echogenic	5/23 (21.7)	7/15 (46.7)	
Mixed	6/23 (26.1)	4/15 (26.7)	
MRI T1 signal, n (%)			
Low	4/9 (44.4)	6/6 (100.0)	0.044*
High	5/9 (55.6)	0/6 (0)	
MRI T2 signal, n (%)			
Low	1/12 (8.3)	0/8 (0)	0.999
High	11/12 (91.7)	8/8 (100.0)	
MRI blood products, n (%)			
Yes	5/19 (26.3)	0/13 (0)	0.064
No	14/19 (73.7)	13/13 (100.0)	

Data are presented as n (%) or median (interquartile range). Denominators are presented for variables with missing data. p values were calculated using Fisher's exact test or the Wilcoxon rank-sum test. * Statistically significant at $p \leq 0.05$.

ondary to cardiac dysfunction in the setting of a possible genetic syndrome. Out of the 38 children who did not regress prenatally, 22 (57.9%) regressed postnatally, 6 (15.8%) underwent surgical resection, 1 (2.6%) was treated with targeted chemotherapy, and 9 (23.7%) underwent continued observation without symptom development. Median time to postnatal regression from birth was 20.1 weeks (IQR: 3.4, 63.0). Median age at surgery was 11.7 weeks (IQR: 1.7, 26.6). Of the 9 children who did not regress or undergo therapy, 6 (66.7%) had lesions that decreased in size over serial postnatal imaging, 1 (11.1%) had a stable lesion over serial postnatal imaging, and 2 (22.2%) were lost to follow-up after the initial postnatal imaging was obtained.

Regarding the most common diagnoses, 2 pulmonary sequestrations regressed postnatally, 3 underwent resection, and 7 were followed up. Two adrenal hemorrhages regressed prenatally, 9 regressed postnatally, and 1 was followed up.

A Kaplan-Meier curve depicting the probability of experiencing lesion regression time after the prenatal diagnosis for all lesions is shown in Figure 4. The Kaplan-Meier estimate for the probability of regression was 47.5% (95% CI: 33.3, 64.2%) at 1 year, 71.7% (95% CI: 55.7, 85.9%) at 2 years, and 75.3% (95% CI: 59.3, 88.6%) at 3 years after prenatal diagnosis. Log-rank testing demonstrated significantly increased probability of regression in lesions without a prenatal feeding vessel (p = 0.006; shown in Fig. 5). All prenatal imaging findings were compared between lesions with and without regression in Table 2. When comparing all 44 lesions on univariate analysis, the presence of a prenatal feeding vessel and low T1 signal on prenatal MRI, characteristics of pulmonary sequestrations, were significantly associated with lesion persistence (p = 0.003; p = 0.044).

Discussion/Conclusion

Prenatally diagnosed suprarenal lesions represent diverse pathologies with varied prognoses, ranging from benign to malignant [6, 8, 10]. Similarly, there is a wide spectrum in the anticipated clinical trajectory of these lesions from spontaneous regression to requiring surgical resection. For example, adrenal hemorrhage represents a benign diagnosis that often resolves spontaneously with conservative management [6]. In contrast, congenital neuroblastoma represents a lesion with variable prognosis, ranging from requiring resection or chemotherapy to undergoing spontaneous regression without intervention [1, 13]. While infradiaphragmatic extralobar pulmonary sequestration is a benign lesion that is asymptomatic, it may require surgical resection in the setting of an unclear diagnosis versus continued observation [6, 7, 14]. The ability to differentiate between these specific diagnoses based upon prenatal imaging features remains challenging, complicating prenatal counseling regarding the lesion's anticipated clinical course. Therefore, this study evaluated prenatal imaging findings associated with specific diagnoses and regression patterns with the goal of refining prenatal counseling in this setting.

We report several prenatal ultrasound and MRI findings that were significantly associated with the diagnosis of a pulmonary sequestration in comparison to adrenal hemorrhage, which were the most common assigned diagnoses in our suprarenal lesions. In contrast to adrenal hemorrhages, pulmonary sequestrations were uniformly left-sided in this series, which is consistent with prior studies reporting a high frequency of left-sidedness [5, 15]. Moreover, pulmonary sequestrations were more likely to be diagnosed earlier in gestation and have specific imaging features including a feeding vessel, solid composition with an echogenic appearance on ultrasound, and low T1 MRI signal. In contrast, adrenal hemorrhages were more likely to have a cystic component on ultrasound and high T1 signal and blood products on MRI. In particular, the T1 MRI characteristics help distinguish sequestration versus adrenal hemorrhage given that adrenal hemorrhages typically have high T1 signal seen with blood products. However, this finding alone does confirm adrenal hemorrhage. Integration of these prenatal findings from both imaging modalities may aid in differentiating these 2 lesions.

While prior studies have explored the utility of prenatal imaging to differentiate the aforementioned diagnoses from neuroblastoma [5, 9, 11], there were only 4 lesions that were assigned a diagnosis of neuroblastoma in this study, which limited comparative analysis. The neuroblastoma lesions were diagnosed later in gestation than the other lesions, which is consistent with prior reports [5], though small sample size precluded statistical comparison with adrenal hemorrhage or pulmonary sequestration. Notably, 1 neuroblastoma confirmed on tissue pathology did have a prenatal feeding vessel, a finding that has been reported in a prior study [2]. Of the 4 neuroblastomas, 1 underwent surgery and 1 underwent chemotherapy. The other 2 lesions classified as neuroblastomas underwent prenatal regression and postnatal regression, respectively, corroborating reports of spontaneous regression in some cases of congenital neuroblastoma [13]. In addition, we also report 2 cases of duplication cysts, which were left-sided, cystic, and anechoic on prenatal ultrasound. Both of these children remained asymptomatic but underwent resection in order to prevent risk of future complications [16, 17].

The majority of all lesions in this study underwent spontaneous regression either prenatally or postnatally. The maximum dimension of lesions at first abnormal prenatal ultrasound was not associated with likelihood of regression. Similarly, the prenatal evolution of lesion size was not associated with likelihood of postnatal regression. Postnatally, the probability of lesion regression was approximately 48% at 1 year and 75% at 3 years after the prenatal diagnosis. Lesion persistence was significantly more likely to occur in the presence of a prenatal feeding vessel and low T1 signal, which were features associated with the diagnosis of a pulmonary sequestration. All children with pulmonary sequestration in this study remained asymptomatic and were either observed until the last follow-up or underwent surgical resection due to unclear diagnosis. Two pulmonary sequestrations in this series were no longer visible on the last postnatal imaging and were categorized as undergoing postnatal regression. These findings are consistent with previous reports highlighting the current recommendation of conservative management of these lesions [14, 18–20].

Limitations

This retrospective study is limited due to its dependence upon chart review for data extraction. Given that the majority of lesions did not undergo biopsy or surgery to obtain a definitive tissue diagnosis, lesions were assigned a diagnosis based upon interpretation of prenatal and postnatal imaging reports and clinical documentation. Since these diagnoses could not be confirmed with tissue pathology, possible bias cannot be excluded. Moreover, small sample sizes within the assigned diagnosis groups other than pulmonary sequestration and adrenal hemorrhage precluded further statistical comparisons

between diagnosis categories. Last, both centers in this study have specialized fetal radiologists, such that these findings may not be generalizable to all centers.

Conclusions

Several prenatal ultrasound and MRI findings may aid in the specific diagnosis of suprarenal lesions, including differentiating pulmonary sequestrations from adrenal hemorrhages. In particular, pulmonary sequestrations were significantly more likely to be left-sided, present earlier in gestation, have a prenatal feeding vessel, and have low T1 MRI signal compared to adrenal hemorrhages. The majority of lesions underwent spontaneous regression, either prenatally or postnatally. A prenatal feeding vessel and low T1 MRI signal, typically indicative of pulmonary sequestrations, were associated with lack of lesion regression. These findings may refine prenatal counseling strategies regarding the most likely diagnosis and expected clinical trajectory of a prenatally identified suprarenal lesion.

Statement of Ethics

This work was performed in compliance with guidelines for human studies and was conducted ethically in accordance with the World Medical Association Declaration of Helsinki. The Institutional Review Board at Boston Children's Hospital and Brigham and Women's Hospital approved this work and did not require informed consent (protocol number P00033073).

Conflict of Interest Statement

The authors have no conflicts of interest to declare.

Funding Sources

The authors did not receive any funding.

Author Contributions

S.L.: data collection, data analysis, manuscript drafting, and manuscript review. D.R.: data collection, data analysis, manuscript drafting, and manuscript review. B.D.: data collection and manuscript review. S.S.: data analysis and manuscript review. C.B.: study design, data analysis, and manuscript review. T.B.: study design, data analysis, and manuscript review.

References

1 Nadler EP, Barksdale EM. Adrenal masses in the newborn. Semin Pediatr Surg. 2000;9(3):156–64.
2 Flanagan SM, Rubesova E, Jaramillo D, Barth RA. Fetal suprarenal masses: assessing the complementary role of magnetic resonance and ultrasound for diagnosis. Pediatr Radiol. 2016;46(2):246–54.
3 Chen CP, Shih SL, Chuang CY, Sheu JC, Chen BF. In utero adrenal hemorrhage: clinical and imaging findings. Acta Obstet Gynecol Scand. 1998;77(2):239–41.
4 Mittelstaedt CA, Volberg FM, Merten DF, Brill PW. The sonographic diagnosis of neonatal adrenal hemorrhage. Radiology. 1979;131(2):453–7.
5 Curtis MR, Mooney DP, Vaccaro TJ, Williams JC, Cendron M, Shorter NA, et al. Prenatal ultrasound characterization of the suprarenal mass: distinction between neuroblastoma and subdiaphragmatic extralobar pulmonary sequestration. J Ultrasound Med. 1997;16(2):75–83.
6 Schwab ME, Braun HJ, Padilla BE. Imaging modalities and management of prenatally diagnosed suprarenal masses: an updated literature review and the experience at a high volume Fetal Treatment Center. J Matern Fetal Neonatal Med. 2020 Jan 26:1–8.
7 Ballouhey Q, Abbo O, Baunin C, Pasquet M, Sartor A, Vayssiere C, et al. Pulmonary and intestinal congenital anomalies masquerading as cystic suprarenal masses. Eur J Pediatr Surg. 2012;22(6):434–8.
8 Maki E, Oh K, Rogers S, Sohaey R. Imaging and differential diagnosis of suprarenal masses in the fetus. J Ultrasound Med. 2014;33(5):895–904.
9 Eo H, Kim JH, Jang KM, Yoo SY, Lim GY, Kim MJ, et al. Comparison of clinico-radiological features between congenital cystic neuroblastoma and neonatal adrenal hemorrhagic pseudocyst. Korean J Radiol. 2011;12(1):52–8.
10 Castro P, Paula Matos A, Werner H, Fazecas T, Nogueira R, Daltro P, et al. Prenatal diagnosis of suprarenal mass by magnetic resonance imaging: a case series. J Matern Fetal Neonatal Med. 2019;32(22):3882–6.
11 de Luca JL, Rousseau T, Durand C, Sagot P, Sapin E. Diagnostic and therapeutic dilemma with large prenatally detected cystic adrenal masses. Fetal Diagn Ther. 2002;17(1):11–6.
12 Moon SB, Shin HB, Seo JM, Lee SK. Clinical features and surgical outcome of a suprarenal mass detected before birth. Pediatr Surg Int. 2010;26(3):241–6.
13 Granata C, Fagnani AM, Gambini C, Boglino C, Bagnulo S, Cecchetto G, et al. Features and outcome of neuroblastoma detected before birth. J Pediatr Surg. 2000;35(1):88–91.
14 Robson VK, Shieh HF, Wilson JM, Buchmiller TL. Non-operative management of extralobar pulmonary sequestration: a safe alternative to resection? Pediatr Surg Int. 2020;36(3):325–31.
15 Xu G, Zhou J, Zeng S, Zhang M, Ouyang Z, Zhao Y, et al. Prenatal diagnosis of fetal intraabdominal extralobar pulmonary sequestration: a 12-year 3-center experience in China. Sci Rep. 2019;9(1):943.
16 Sujka JA, Sobrino J, Benedict LA, Alemayehu H, Peter SS, Hendrickson R. Enteric duplication in children. Pediatr Surg Int. 2018;34(12):1329–32.
17 Fahy AS, Pierro A. A systematic review of prenatally diagnosed intra-abdominal enteric duplication cysts. Eur J Pediatr Surg. 2019;29(1):68–74.
18 Obeidat N, Sallout B, ALAAli W. Isolated subdiaphragmatic extralobar pulmonary sequestration: masquerading as suprarenal mass with spontaneous resolution. Clin Exp Obstet Gynecol. 2016;43(3):457–9.
19 ALAAli P, Lucaya J, Hendry GM, McAndrew PT, Duran C. Spontaneous involution of pulmonary sequestration in children: a report of two cases and review of the literature. Pediatr Radiol. 1998;28(4):266–70.
20 Chowdhury M, Samuel M, Ramsay A, Constantinou J, McHugh K, Pierro A. Spontaneous postnatal involution of intraabdominal pulmonary sequestration. J Pediatr Surg. 2004;39(8):1273–5.